

Pauli-principle driven correlations in four-neutron nuclear decays

P.G. Sharov,^{1,*} L.V. Grigorenko,^{1,2,3} I. Mukha,⁴ A. Ismailova,¹ and M.V. Zhukov⁵

¹*Flerov Laboratory of Nuclear Reactions, JINR, 141980 Dubna, Russia*

²*National Research Nuclear University “MEPhI”, 115409 Moscow, Russia*

³*National Research Centre “Kurchatov Institute”, Kurchatov sq. 1, 123182 Moscow, Russia*

⁴*GSI Helmholtzzentrum für Schwerionenforschung GmbH, 64291 Darmstadt, Germany*

⁵*Department of Physics, Chalmers University of Technology, 41296 Göteborg, Sweden*

Mechanism of simultaneous non-sequential four-neutron ($4n$) emission (or “true” $4n$ -decay) has been considered in five-body approach. It demonstrates that $4n$ -decay fragments should have specific energy and angular correlations reflecting strong spacial correlations of “valence” neutrons orbiting in their $4n$ -precursors. Due to the Pauli exclusion principle, the valent neutrons are pushed to the symmetry-allowed configurations in the $4n$ -precursor structure, which causes a “Pauli focusing” effect. Prospects of observation of the Pauli focusing have been considered for the $4n$ precursors ^7H and ^{28}O . Fingerprints of their nuclear structure or/and decay dynamics are predicted.

PACS numbers: 27.20.+n, 21.65.Cd, 21.45.-v, 25.70.Pq, 23.20.En

Introduction. — In the last decade there was a great progress in the studies of three-body decays (e.g. two-proton radioactivity) [1]. In contrast with “conventional” two-body decays, for three-body decays a lot of additional information is encrypted in the momentum (energy and angular) correlations. Theoretical studies indicate that both effects of the initial nuclear structure and the decay mechanism can show up in the correlation patterns in various ways [2–9].

With development of experimental techniques more and more “complicated” nuclear systems become available for studies. One of such complicated cases are isotonic neighbors of the $4n$ halo systems located beyond the neutron dripline and decaying via $4n$ emission. Examples of such systems which are now actively challenged by experiment are ^7H and ^{28}O . The phenomenon is expected to be widespread beyond the neutron dripline and other possible candidates for such a decay mode, e.g. ^{18}Be can be mentioned. Their ground states are expected to be unbound with $E_T \lesssim 2$ MeV (E_T is energy above the $4n$ decay threshold), and the decay mechanism can be so-called “true” $4n$ emission: there are no sequential neutron emission processes, and all neutrons are emitted simultaneously. For low decay energies $E_T \lesssim 100$ –300 keV such a decay mechanism may lead to very long lifetimes characterized in terms of $4n$ radioactivity [10]. From experimental side only $4p$ emission from ^8C has been studied so far [11]. However, this decay has sequential $^8\text{C} \rightarrow 2p + (^6\text{Be} \rightarrow 2p + \alpha)$ character.

It is clear that for $4n$ emission the five-body correlations encrypt enormously more information compared to the three-body case: the complete correlation pattern is described by 11-dimensional space compared to the 2-dimensional one. The decay amplitude antisymmetrization should decrease the effective dimension of the correlation space, but there should be still a lot. The question

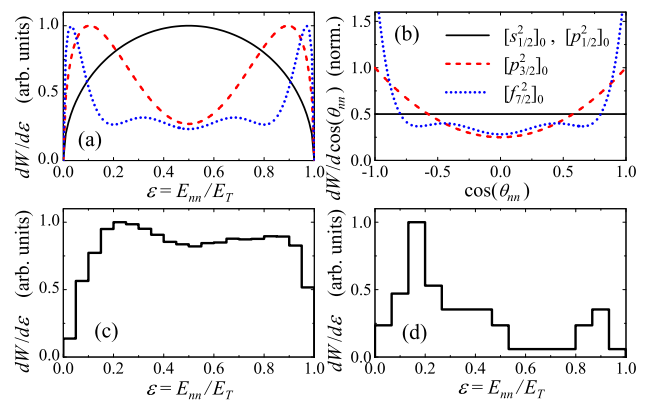


FIG. 1. (color online) Pauli focusing for three-body decays with valence $2n$ in configurations $[s_{1/2}^2]_0$, $[p_{1/2}^2]_0$, $[p_{3/2}^2]_0$, and $[f_{7/2}^2]_0$. Panel (a) shows n - n energy distribution, panel (b) shows n - n angular distribution obtained neglecting n - n final state interaction. Panels (c) and (d) show energy p - p distributions observed for ^6Be [5] and ^{45}Fe [12].

which can be asked here is “What are physically meaningful signals in this wealth of information?”

This work demonstrates that core- n and n - n energy and angular distributions may provide important information on the dominant configurations involved in the $4n$ decay. Moreover, the studies of correlated $\{i - j, k - l\}$ patterns of energy and angular distributions may give unique signatures for orbital configurations involved in the decay (numbers $i \neq j$, $k \neq l$ enumerate different selections of decay products)

The concept of “Pauli focusing” was proposed in [13] and further discussed e.g. in [14, 15] for the bound state structure of three-body core+ n + n systems. It was demonstrated that due to Pauli principle population of orbital configurations $[l_{j_1} \otimes l_{j_2}]_J$ for the valence nucleons may induce strong spatial correlations depending on specific values of j_1 , j_2 , and J . Various forms of such correlations were actively discussed as integral part of the

* sharovpavel@jinr.ru

two-nucleon halo phenomenon.

For bound states the theoretically predicted Pauli focusing correlations are “hidden” in the nuclear interior and can be accessed experimentally only in some indirect way. In contrast, in the three-body decay process these internal correlations may directly exhibit themselves in the momentum distributions of the decay products. This is illustrated in Fig. 1 for the three-body decays of the orbital configurations $[s_{1/2}]_0$ and $[p_{1/2}]_0$ (corresponds to phase-space $\sqrt{\varepsilon(1-\varepsilon)}$ and isotropy), $[p_{3/2}]_0$ and $[f_{7/2}]_0$ (strong $2n$ correlations). This situation is also illustrated by the experimentally observed energy distributions of fragments in the $2p$ decays of ${}^6\text{Be}$ and ${}^{45}\text{Fe}$. Qualitatively, the signature of the Pauli focusing, the double-hump structure characteristic for $[p_{3/2}]_0$, can be easily seen. However, for quantitative consideration two effects should be considered: (i) nucleon-nucleon final state interaction (FSI) and (ii) subbarrier tunneling to configurations with lower angular momenta (and hence easier penetration). For corresponding discussions, see Refs. [1, 4, 6]. In the process of penetration through the subbarrier region the following changes in the orbital populations take place

$${}^6\text{Be} : \quad [p_{3/2}]_0 \rightarrow C_{23}[p_{3/2}]_0 + C_{01}[s_{1/2}]_0, \quad (1)$$

$${}^{45}\text{Fe} : \quad [f_{7/2}]_0 \rightarrow C_{67}[f_{7/2}]_0 + C_{23}[p_{3/2}]_0. \quad (2)$$

The complete three-body model studies give $C_{23} \approx C_{01}$ in ${}^6\text{Be}$ and $C_{67} \ll C_{23}$ in ${}^{45}\text{Fe}$, explaining the difference in qualitative and quantitative description of spectra.

Pauli focusing for 5-body systems was discussed in [16] by example of ${}^8\text{He}$ nucleus in the $\alpha+4n$ model. The same case was considered in much more details in [17]. In analogy with three-body case we may expect that Pauli focusing correlations found in the bound five-body system should exhibit themselves in decays if such a systems are located above the five-body breakup threshold. However, the questions *whether* and *how* such correlations can be used to extract physical information have never been discussed so far.

phase-space distributions. — Before we consider a physically meaningful signal we should first understand the “kinematically defined” correlations, which are connected with phase-space of several particles. The phase-space V_4 for 5 particles can be defined by 4 energies $E_i = \varepsilon_i E_T$ corresponding to 4 Jacobi vectors in the momentum space

$$dV_4 \sim \delta(E_T - \sum_i \varepsilon_i E_T) \sqrt{\varepsilon_1 \varepsilon_2 \varepsilon_3 \varepsilon_4} d\varepsilon_1 d\varepsilon_2 d\varepsilon_3 d\varepsilon_4. \quad (3)$$

The phase-space energy distribution between any two fragments $dV_1/d\varepsilon_1$ and correlated phase-space distribution of two energies $dV_{12}/d\varepsilon_1 d\varepsilon_2$ can be obtained by the respective integrations of Eq. (3)

$$dV_1 \sim \sqrt{(1-\varepsilon_1)^7 \varepsilon_1} d\varepsilon_1, \quad (4)$$

$$dV_{12} \sim (1-\varepsilon_1 - \varepsilon_2)^2 \sqrt{\varepsilon_1 \varepsilon_2} d\varepsilon_1 d\varepsilon_2, \quad (5)$$

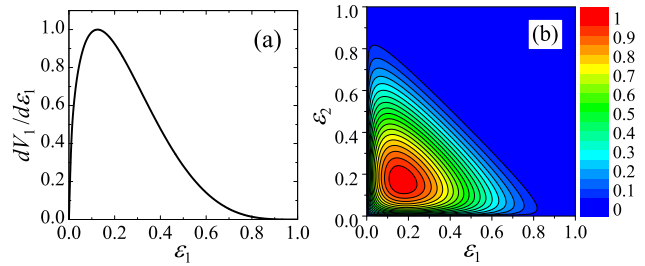


FIG. 2. (color online) Five-body phase-space (a) one- and (b) two-dimensional energy distributions of Eqs. (4) and (5).

see also Fig. 2. The distribution (4) has a maximum at $\varepsilon_1 = 1/8$ and a mean energy value $\varepsilon_1 = 1/4$.

In addition to the one-dimensional distributions of Eq. (4), the correlated two-dimensional $\{i-k, n-m\}$ ($i \neq k$, $n \neq m$) energy and angular distributions may be constructed. For core+4n decays in total five topologically nonequivalent such distributions exist, see Fig. 3. It is evident that “topologically disconnected” distributions $cn-nn$ and $nn-nn$ are equivalent to distributions of Eq. (5) and Fig. 2 (b) as Jacobi variables are “disconnected” in the same sense. It can be seen that the other correlated distributions have quite distinctive shapes even in the phase-space case.

Model for dynamics of 5-body decay. — The differential decay probability is defined as

$$dW \sim |T|^2 dV_4 \prod_{i=1..4} d\Omega_i.$$

The decay amplitude for core+ $n_1+n_2+n_3+n_4$ decay is approximated by expression

$$T = \mathcal{A} [\prod_{i=1..4} A_{cn_i}(l_i, j_i, \mathbf{p}_{cn_i})]_J, \quad (6)$$

where \mathbf{p}_{cn_i} , l_i and j_i are momentum, angular momentum, and total spin conjugated to radius-vector \mathbf{r}_{cn_i} between core and nucleon number i . The amplitude considered to have define total spin J is antisymmetrized (operator \mathcal{A} above) for permutation of four valence nucleons. The Monte-Carlo procedure is used to compute various momentum distributions. The single-particle amplitudes are approximated by \mathfrak{R} -matrix type expression

$$A_{cn_i}(l_i, j_i, \mathbf{p}_{cn_i}) = \frac{1}{2} \frac{a_{l_i j_i} \sqrt{\Gamma_{cn_i}(E_{cn_i})}}{E_{r,cn_i} - E_{cn_i} - i\Gamma_{cn_i}(E_{cn_i})/2}, \quad (7)$$

where E_{r,cn_i} is resonance energy in the cn_i channel, while $\Gamma_{cn_i}(E_{cn_i})$ is its standard \mathfrak{R} -matrix width as a function of energy. This reasonable approximation becomes very precise in the limit of infinite core mass.

To estimate the possible effect of n - n FSI, the Eq. (6) can be modified as

$$T = \mathcal{A} [\prod_{i=1..4} A_{cn_i}(\mathbf{p}_{cn_i}) \prod_{i>k} A_{n_i n_k}(\mathbf{p}_{n_i n_k})]. \quad (8)$$

The amplitude $A_{n_i n_k}$ is the (typical for the Migdal-Watson-type approximations) zero-range expression for

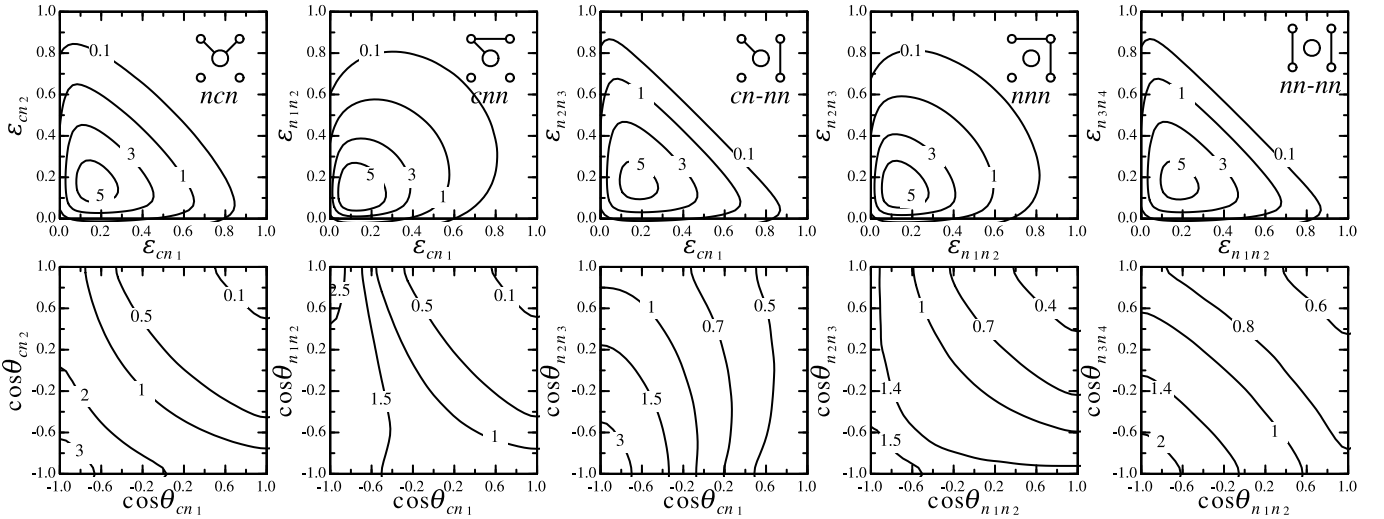


FIG. 3. Nonequivalent five-body phase-space correlated energy (upper row) and angular (lower row) distributions for *core+4n* decays. The sketches in the upper row panels illustrate the selection of correlated pairs of fragments: *ncn*, *cnn*, *cn-nn*, *nnn*, *nn-nn*.

an *s*-wave *n-n* scattering

$$A_{n_i n_k} = \frac{a_s}{1 - i p_{n_i n_k} a_s}, \quad (9)$$

where $a_s = -18.9$ fm is the scattering length in the *n-n* channel. This approximation provides no control of actual total spin in the particular n_i - n_k channel. Thus the effect of *n-n* FSI should be much overestimated here as, *on average*, only two pairs of neutrons (out of six possible selections) can be both in relative $s = 0$ state and in relative *s*-wave simultaneously. So, we may consider Eq. (8) as an upper-limit estimate of the effect.

Scenarios of 5-body decay. — The five-body decays are so far not studied. Thus, in our discussion we follow the assumed qualitative analogy of 3-body and 5-body decay dynamics. Let us consider the examples of ^7H and ^{28}O whose internal structure is expected to be dominated by $[p_{3/2}]_0$ and $[d_{3/2}]_0$ configurations respectively. In the process of decay these configurations may drift to configurations with lower angular momenta in analogy with Eqs. (1) and (2)

$$^7\text{H}: [p_{3/2}]_0 \rightarrow C_{2323}[p_{3/2}]_0 + C_{0123}[s_{1/2}^2 p_{3/2}]_0, \quad (10)$$

$$^{28}\text{O}: [d_{3/2}]_0 \rightarrow C_{4343}[d_{3/2}]_0 + C_{0143}[s_{1/2}^2 d_{3/2}]_0 + C_{0123}[s_{1/2}^2 p_{3/2}]_0. \quad (11)$$

The one-dimensional energy and angular distributions for the pure above-mentioned configurations in the *core-n* and *n-n* channels are shown in Fig. 4. On average, the increase of angular momentum “content” of the component leads to the increase of the mean energy in the *core-n* and the corresponding decrease in the *n-n* channels. The respective angular distributions have quite distinctive patterns. So, one may see a strong effect of definite orbital configuration already in these observables.

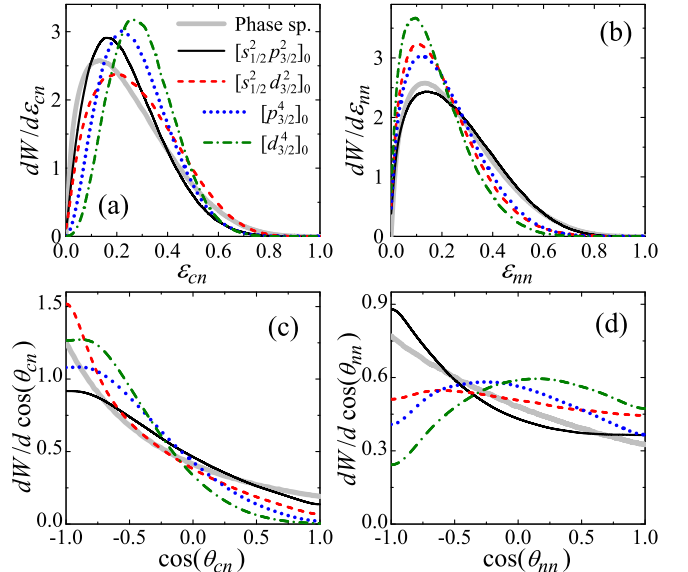


FIG. 4. (color online) Normalized energy (a,b) and angular (c,d) distributions in the *core-n* (a,c) and *n-n* (b,d) channels of 4n-decay for different pure 4n configurations present in Eqs. (10) and (11). The decay energy $E_T = 500$ keV. The reference phase-space distribution is shown by the thick gray line.

The Pauli focusing effect on two-dimensional correlated energy distributions is illustrated in Fig. 5 (col. 1) for one selected *nn-nn* topology. All four considered cases are quite distinguishable from the phase-space distributions, as well as from each other. Among them the case of $[s_{1/2}^2 p_{3/2}]_0$ configuration has a strong qualitative distinction. Even stronger variability can be seen in the correlated angular distributions, which are systematically surveyed in Fig. 5 (cols. 2–6). The correlation patterns

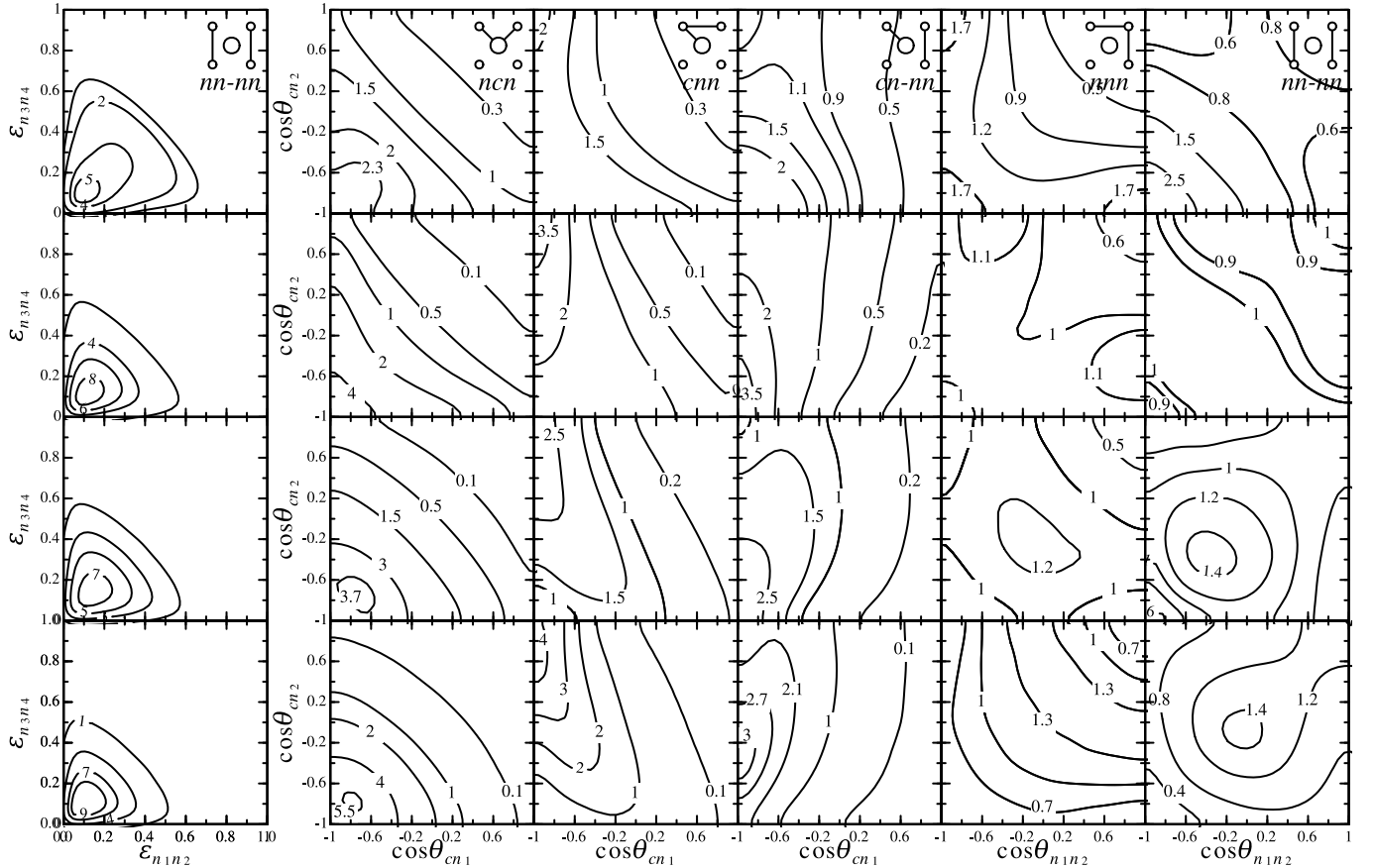


FIG. 5. Correlated energy distributions for $nn-nn$ topology (col. 1) and correlated angular distributions for ncn (col. 2), cnn (col. 3), $cn-nn$ (col. 4), nnn (col. 5), and $nn-nn$ (col. 6) topologies. Configurations from Eqs. (10) and (11) correspond to the pure components $[s_{1/2}^2 p_{3/2}]_0$ (row 1), $[s_{1/2}^2 d_{3/2}]_0$ (row 2), $[p_{3/2}]_0$ (row 3), and $[d_{3/2}]_0$ (row 4). The decay energy $E_T = 500$ keV.

show great variability: all of them are strongly different from the phase-space distributions and from each other. Therefore the predicted correlation patterns provide clear signatures on dominating $4n$ -decay configurations, which may be used in data analysis of future experiments.

Discussion. — The experience of three-body decay studies tell us that the effect of configuration mixing in the final state may have strong effect on the observed correlations. However, the simplified predicted correlations may be relevant in two limiting cases. (i) For decay energies above the typical barrier energies (e.g. $E_T > 2 - 4$ MeV) the effect of configuration mixing may be small, and then one-configuration approximation may be precise enough. However, n - n FSI should have growing effect on the distributions in such a limiting case. (ii) For deep subbarrier energies $E_T < 100 - 300$ keV, the decay should proceed via the $[s^2 p^2]_0$ configurations which have the lowest possible barriers. For the case (ii) our predictions should be very precise with improving precision in the limit $E_T \rightarrow 0$.

Effect of n - n FSI is known to strongly influence the three-body energy and angular correlations. In three-body case this effect is expected to vanish as decay energy goes below $E_T \sim 100$ keV, see, e.g. [9]. Distributions of

Fig. 6 obtained by Eq. (8) for $[s_{1/2}^2 p_{3/2}]$ configuration illustrate how important can be the effect of n - n FSI in five-body decay. We can see that the effect is reasonably small under $E_T < 300$ keV and can be neglected under $E_T < 100$ keV. Curious to note that the modifications of the n - n energy distribution by the n - n FSI for $E_T < 1$ MeV is very well described by the Migdal-Watson type expression

$$\frac{dW}{d\varepsilon_{nn}} = \frac{dW_{ps}}{d\varepsilon_{nn}} \frac{a_s^2(\text{eff})}{1 + 2M_{nn} E_T \varepsilon_{nn} a_s^2(\text{eff})}, \quad (12)$$

where $dW_{ps}/d\varepsilon_{nn}$ is the phase-space distribution and $a_s(\text{eff}) = -11.5$ fm is a sort of effective scattering length, see thin solid curve in Fig. 6 (b). Thus we can qualitatively state that the effective length of the n - n FSI within the emitted in the decay of such configuration “tetra-neutron” is around 44% of the “vacuum value” with $a_s = -18.9$ fm.

Conclusion. — In this work we have for the first time theoretically studied the correlations in emission of four neutrons in the nuclear 5-body decay. We have demonstrated that for true five-body decays of core+ $4n$ systems the *Pauli focusing* — the cumulative effects of antisym-

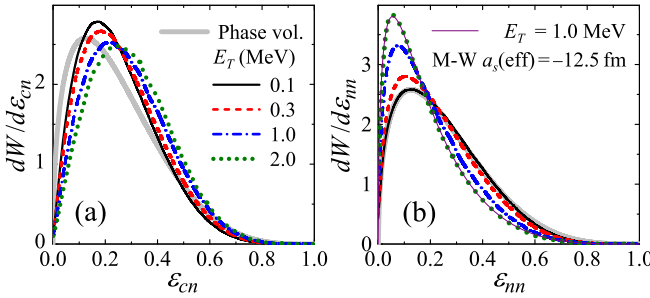


FIG. 6. (color online) Effect of n - n FSI on energy distributions in core- n (a) and n - n (b) channels at different decay energies E_T for $[s_{1/2}^2 p_{3/2}^2]$ configuration. Solid, dashed, and dotted lines correspond to E_T of 0.1, 0.3, and 1.0 MeV, respectively. Phase-space is shown by thick grey line.

metrization and population of definite orbital configurations — may lead to distinctive correlation patterns. We propose to measure two-dimensional correlated energy or/and angular distributions for derivation of information concerning the quantum-mechanical $4n$ -decay configuration. In total five distinct correlated distributions are available for analysis and they seem to form a unique “fingerprint” of the decay quantum state.

Acknowledgments. — This work for PGS and LVG was supported in part by the Russian Science Foundation grant No. 17-12-01367.

[1] M. Pfützner, M. Karny, L. V. Grigorenko, and K. Riisager, Rev. Mod. Phys. **84**, 567 (2012).

[2] L. V. Grigorenko and M. V. Zhukov, Phys. Rev. C **68**, 054005 (2003).

[3] L. V. Grigorenko, T. D. Wiser, K. Miernik, R. J. Charity, M. Pfützner, A. Banu, C. R. Bingham, M. Cwiok, I. G. Darby, W. Dominik, J. M. Elson, T. Ginter, R. Grzywacz, Z. Janas, M. Karny, A. Korgul, S. N. Liddick, K. Mercurio, M. Rajabali, K. Rykaczewski, R. Shane, L. G. Sobotka, A. Stolz, L. Trache, R. E. Tribble, A. H. Wuosmaa, and M. V. Zhukov, Phys. Lett. B **677**, 30 (2009).

[4] L. V. Grigorenko, T. D. Wiser, K. Mercurio, R. J. Charity, R. Shane, L. G. Sobotka, J. M. Elson, A. H. Wuosmaa, A. Banu, M. McCleskey, L. Trache, R. E. Tribble, and M. V. Zhukov, Phys. Rev. C **80**, 034602 (2009).

[5] I. A. Egorova, R. J. Charity, L. V. Grigorenko, Z. Chajecki, D. Coupland, J. M. Elson, T. K. Ghosh, M. E. Howard, H. Iwasaki, M. Kilburn, J. Lee, W. G. Lynch, J. Manfredi, S. T. Marley, A. Sanetullaev, R. Shane, D. V. Shetty, L. G. Sobotka, M. B. Tsang, J. Winkelbauer, A. H. Wuosmaa, M. Youngs, and M. V. Zhukov, Phys. Rev. Lett. **109**, 202502 (2012).

[6] L. V. Grigorenko, I. G. Mukha, and M. V. Zhukov, Phys. Rev. Lett. **111**, 042501 (2013).

[7] K. W. Brown, R. J. Charity, L. G. Sobotka, Z. Chajecki, L. V. Grigorenko, I. A. Egorova, Y. L. Parfenova, M. V. Zhukov, S. Bedoor, W. W. Buhro, J. M. Elson, W. G. Lynch, J. Manfredi, D. G. McNeel, W. Reviol, R. Shane, R. H. Showalter, M. B. Tsang, J. R. Winkelbauer, and A. H. Wuosmaa, Phys. Rev. Lett. **113**, 232501 (2014).

[8] K. W. Brown, R. J. Charity, L. G. Sobotka, L. V. Grigorenko, T. A. Golubkova, S. Bedoor, W. W. Buhro, Z. Chajecki, J. M. Elson, W. G. Lynch, J. Manfredi, D. G. McNeel, W. Reviol, R. Shane, R. H. Showalter, M. B. Tsang, J. R. Winkelbauer, and A. H. Wuosmaa, Phys. Rev. C **92**, 034329 (2015).

[9] L. V. Grigorenko, J. S. Vaagen, and M. V. Zhukov, Phys. Rev. C **97**, 034605 (2018).

[10] L. V. Grigorenko, I. G. Mukha, C. Scheidenberger, and M. V. Zhukov, Phys. Rev. C **84**, 021303(R) (2011).

[11] R. J. Charity, J. M. Elson, J. Manfredi, R. Shane, L. G. Sobotka, B. A. Brown, Z. Chajecki, D. Coupland, H. Iwasaki, M. Kilburn, J. Lee, W. G. Lynch, A. Sanetullaev, M. B. Tsang, J. Winkelbauer, M. Youngs, S. T. Marley, D. V. Shetty, A. H. Wuosmaa, T. K. Ghosh, and M. E. Howard, Phys. Rev. C **84**, 014320 (2011).

[12] K. Miernik, W. Dominik, Z. Janas, M. Pfützner, L. Grigorenko, C. R. Bingham, H. Czyrkowski, M. Cwiok, I. G. Darby, R. Dabrowski, T. Ginter, R. Grzywacz, M. Karny, A. Korgul, W. Kusmierz, S. N. Liddick, M. Rajabali, K. Rykaczewski, and A. Stolz, Phys. Rev. Lett. **99**, 192501 (2007).

[13] B. Danilin, M. Zhukov, A. Korsheninnikov, V. Efros, and L. Chulkov, Sov. J. Nucl. Phys. **48**, 766 (1988), [Yad. Fiz. 48, 1208 (1988)].

[14] M. V. Zhukov, B. Danilin, D. Fedorov, J. Bang, I. Thompson, and J.S. Vaagen, Phys. Rep. **231**, 151 (1993).

[15] P. Mei and P. V. Isacker, Annals of Physics **327**, 1162 (2012).

[16] M. V. Zhukov, A. A. Korsheninnikov, and M. H. Smedberg, Phys. Rev. C **50**, R1 (1994).

[17] P. Mei and P. V. Isacker, Annals of Physics **327**, 1182 (2012).